ELSEVIER

Polymer 42 (2001) 10119–10132

polymer

www.elsevier.com/locate/polymer

A polarised μ-FTIR study on a model system for nylon 6 6: implications for the nylon Brill structure

Sharon J. Cooper[a,*], Mike Coogan[b], Neil Everall[c], Ian Priestnall[c]

[a]*Department of Chemistry, Science Laboratories, University of Durham, South Rd., Durham DH1 3LE, UK*
[b]*Department of Chemistry, Cardiff University, P.O. Box 912, Cardiff CF10 3TB, UK*
[c]*ICI PLC, Wilton Research Centre, P.O. Box 90, Middlesbrough, Cleveland TS90 8JE, UK*

Received 16 March 2001; received in revised form 27 July 2001; accepted 6 August 2001

Abstract

Polarised transmission FTIR microscopy studies (μ-FTIR) have been performed on a monodisperse 3-amide oligomer. The oligomer is a model compound for nylon 6 6; it has essentially the same room temperature crystal structure, and it undergoes the same high temperature transition, the Brill transition, prior to melting. However, the oligoamide forms extended chain, rather than chain-folded, crystals, and so crystals are produced that are essentially 100% crystalline, and of ~μm–mm size. Consequently, this material is ideally suited for polarised μ-FTIR single crystal studies. The thermal polarised FTIR behaviour of this material provides definitive proof that the Brill transition does not involve major rearrangement of hydrogen bonds, since the strong parallel polarisation of both the NH stretch and amide I bands are retained right up to melting. Quantitative infrared dichroism measurements indicate that a maximum of 5° rotation of the N–H bonds about the extended chain axis occurs prior to melting. These results strongly suggests that the equivalent Brill transition in nylon 6 6 also proceeds without significant hydrogen bond rearrangement. In addition we have investigated the behaviour of designated 'Brill', 'crystalline', 'amorphous' and 'fold' bands that are present in our spectra. © 2001 Published by Elsevier Science Ltd.

Keywords: Nylon; Oligoamides; Brill transition

1. Introduction

The nature of the Brill transition in nylons, first reported by Brill [1] in 1942 for nylon 6 6 is still controversial. This solid-state transition occurs upon heating nylon 6 6 and many other nylons. The transition is characterised by a change from a triclinic [2] to pseudohexagonal crystal structure, characterised by the convergence of the two strong interchain diffraction signals at 0.44 and 0.37 nm to an intermediate value of 0.42 nm. Many groups [3–6] believe that the integrity of the hydrogen-bonded sheet structure, present in the room temperature structure, is maintained throughout the Brill transition, and up to the melting point. The main supporting evidence includes (i) an NMR study on deuterium labelled nylon 6 6 in which it was shown that the motion of ND groups could be modelled by assuming restricted librational motion at all temperatures below melting [5] and (ii) X-ray diffraction studies in which it was found that the intersheet interamide distance in the nylon 6 6 pseudohexagonal structure was too great to permit hydrogen bond formation [4]. Other evidence [7–12], however, indicates that the attainment of a pseudohexagonal structure may be driven by a partial rearrangement of hydrogen bonds into intersheet directions, similar to that first postulated by Brill. This model offers a simple explanation for the interchain distances remaining nearly constant at 0.42 nm between the Brill transition temperature, T_B, and the melting point, T_m. Furthermore, crystals with a hexagonal morphology, indicative of similar growth rates (and hence similar intermolecular forces) in three trigonal directions have been obtained for a related oligoamide material. This suggests that a three-dimensional hydrogen bond network has formed [13].

The nature of the Brill transition is also contentious. The Brill transition shows hysteresis, suggestive of a first order process, upon heating and cooling nylon 6 6 [14]. However, the presence of an endothermic peak in DSC traces at T_B has only been identified for crystallisation from solution [14–16]; this has been attributed [15] to the better defined T_B which results from the more uniform crystals obtained by crystallisation from dilute solution, as opposed

* Corresponding author. Tel.: +44-191-374-4638; fax: +44-191-384-4737.
E-mail address: sharon.cooper@durham.ac.uk (S.J. Cooper).

0032-3861/01/$ - see front matter © 2001 Published by Elsevier Science Ltd.
PII: S0032-3861(01)00566-3

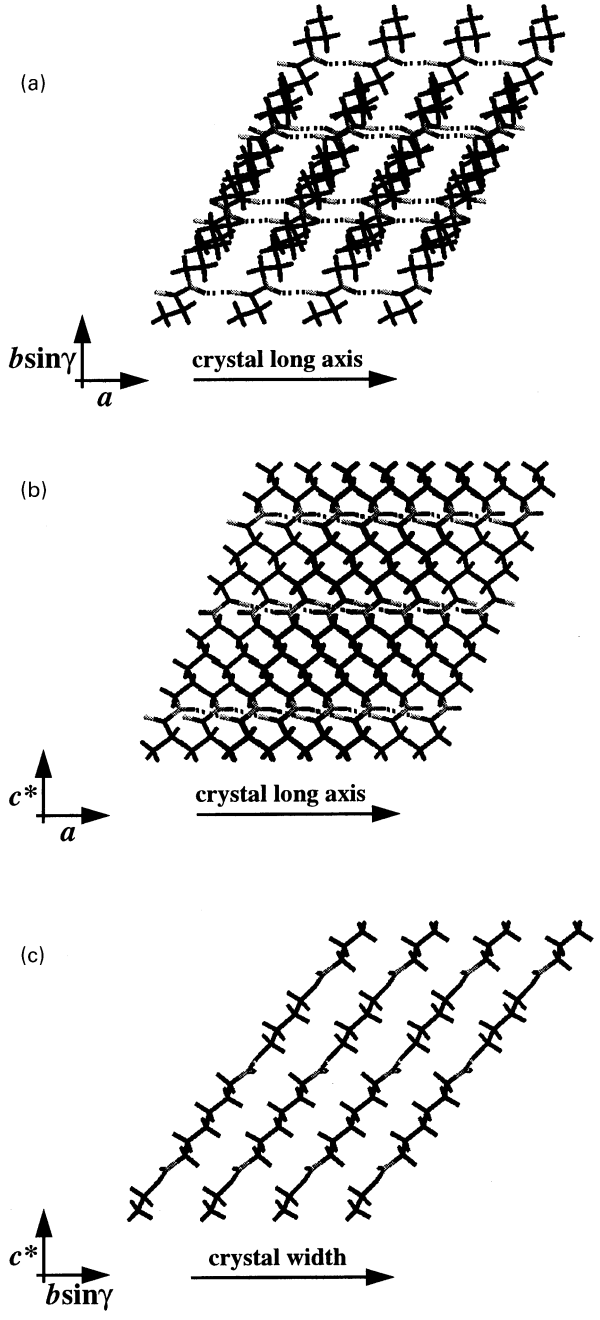

Fig. 1. Views showing the molecular structure within the 3-amide nylon 6 6 crystals. The methylene units are in black, the amide units are in grey and the hydrogen bonds are shown by dashed lines. The crystal thickness, length and width directions run parallel to the c^*, a and b sin γ directions, respectively. (a) Projection along the c^*-direction onto the ab plane showing the hydrogen bonds running along the a-axis. (b) View of the ac^* plane showing the hydrogen bonds parallel to the a-axis. (c) Projection along the a-axis showing the pronounced interchain shear in this plane.

to crystallisation from the melt. The following, though, appears to be generally accepted.

1. The Brill temperature, T_B, at which the transition occurs for a particular nylon depends upon its crystallisation conditions and thermal history. In particular, for melt crystallisation the higher the crystallisation temperature the higher the observed T_B, with T_B values of ~160–225°C reported for nylon 6 6 melt crystallised at temperatures between 196 and 260°C [14]. For nylon 6 6 crystallised from a range of solvents and crystallisation temperatures, T_B values of ~200–220°C have been reported [11,16,17]. These T_B values are higher than those obtained from all but the highest melt crystallisation temperatures, and the values are less dependant upon the crystallisation temperature; these results also reflect the more uniform, single crystal architectures typically obtained by isothermal crystallisation from dilute solution. In contrast, for nylon 6 6 fibres, T_B's are lower at ~160°C [1].
2. The alkane segments undergo large amplitude librational motion above T_B.

The recent use of monodisperse oligoamides as model systems for nylons has been beneficial in gaining insight into nylon behaviour [13,18,19]. Monodisperse oligoamides are unhampered by polydispersity effects and consequently can provide high resolution experimental data. In addition, the shorter length variants form extended chain crystals, so that the crystallinity is essentially 100% and any effects due to chain folding are absent. In this contribution, we have investigated the structural variations with temperature of a three amide oligomer of nylon 6 6 using polarised μ-FTIR.

Previous studies [18,19] have shown several aspects of the behaviour of this 3-amide oligomer to be analogous to that of nylon 6 6. In particular: (i) the room temperature structure is equivalent to that of nylon 6 6; the oligoamide has the same hydrogen-bonded sheet structure and the sheets stack with a progressive shear, see Fig. 1, and (ii) the material undergoes a Brill transition at ~155°C for solution crystallised material, prior to its reported melting at 177°C. Furthermore it was shown [18] that the hydrogen bond direction is (i) coincident with the crystal long axis, and (ii) essentially parallel to the platelet surfaces, which are parallel to the (001) plane (i.e. the c^* axis is vertical, see Fig. 1). At room temperature, the intersheet shear results in the chain axis being inclined at ~40° to the platelet surface normal, with the tilt occurring mainly in the direction of the crystal width (see Fig. 1c). As the crystals are heated up to melting, this chain axis tilt decreases to ~35°. The main difference between this 3-amide oligomer and the nylon 6 6 polymer is that the oligoamide can be crystallised to give extended chain single crystals of essentially 100% crystallinity, i.e. the crystals are free from amorphous and chain-folded regions. It is these features that make the oligoamide crystal particularly suitable for polarised μ-FTIR studies.

There have been numerous FTIR studies on nylon 6 6 and related compounds [20–34]. A number of studies are particularly relevant to the present report. Vasanthan et al. [20] have recently shown that some of the weaker IR bands in the nylon 6 6 spectra disappear abruptly at the Brill transition. A polarised FTIR study was performed by Itoh [21] on a

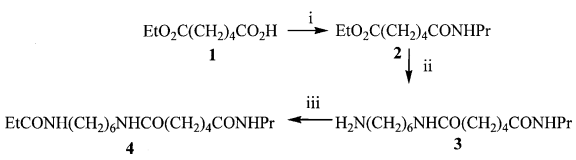

Reagents and conditions:- i)$SOCl_2$ reflux 2h.then propylamine, dichloromethane; ii) 1,6 diaminohexane, neat 100 °C; iii) propionyl chloride, triethylamine, chloroform 30 % 3 steps.

Fig. 2. Synthesis scheme.

biaxial nylon 6 6 film and indicated that the dichroism exhibited by the N–H stretch band at ~3304 cm^{-1} did not decrease on heating from room temperature up to the melting point. Surprisingly, however, the Brill transition was reported to have not occurred for this biaxial specimen, so that the findings cannot be related to typical nylon 6 6 behaviour. Various studies [22–24] have also allocated particular bands to the amorphous, regular chain-folded and crystalline regions of the nylon 6 6 polymer. The objectives of the present FTIR study on this ~100% crystalline 3-amide nylon 6 6 model compound are two-fold. Firstly, to establish whether or not a rearrangement of hydrogen bonds does occur at the Brill transition, and secondly to investigate the extent to which particular IR bands can be assigned to amorphous, fold or crystalline entities.

2. Experimental section

2.1. Materials

The 3-amide oligomer of nylon 6 6 (i.e. 6-propionamidohexyladipamidopropionamide) was synthesised following the scheme shown in Fig. 2. This scheme uses a new approach to the synthesis of oligoamides in order to avoid the lengthy protection–deprotection sequences, which have traditionally been employed. This approach relies upon synthetic steps designed to exploit the lower reactivities of amides compared to both esters and amines to avoid unwanted side reactions without the need for additional protections. Crucially the diamine may be introduced unprotected, and by the simplest of possible procedures; heating neat with the amidoester **2** (see Fig. 2). Thus, from the unsymmetrical adipoyl moiety **1** the newly formed amide unit of **2** acts as its own protection, even under the forcing conditions required to convert the ester to amide **3**. Selective acylation of the primary amine over the amide (which, surprisingly, proved non-trivial under other conditions) gives **4** in an overall yield of 30% which compares well to the yields of oligoamides obtained after multi-step procedures, and is a far simpler synthesis to achieve. Further details are given below.

2.2. Ethyl adipoylpropionamide (*2*)

To monoethyladipate **1** (Aldrich chemical company) (7.55 g, 43 mmol) was added thionyl chloride (5 ml, 8.15 g, 68 mmol) and the mixture heated at reflux for 2 h before excess thionyl chloride and volatile products were removed in vacuo. The residual oil was dissolved in dichloromethane (100 ml) cooled in an ice-bath and a solution of propylamine (10 ml, 120 mmol) in dichloromethane (20 ml) added drop-wise with stirring. After the addition was complete (30 min) the mixture was allowed to attain ambient temperature with stirring over 2 h, then washed with sodium hydrogen carbonate (saturated aqueous, 3×50 ml), brine (saturated, 50 ml) dried ($MgSO_4$) and concentrated in vacuo to give ethyl adipoylpropionamide (**2**) 6.54 g, 71% as a pale yellow oil [35]. This material was of sufficient purity to be used in subsequent steps.

2.3. 6-Aminohexyladipamidopropionamide (*3*)

To ethyl adipoylpropionamide **2** (4 g, 18 mmol) was added 1,6 diaminohexane (20 g, 172 mmol) and the efficiently stirred mixture was heated at 100°C for 16 h. After this period the excess diamine and volatile products were removed (100°C/15 mm Hg 1 h with stirring) and the residual oil precipitated with diethyl ether. Crystallisation of the crude product from dichloromethane by addition of diethyl ether gave 6-aminohexyladipamidopropionamide (**3**), 3.2 g 62% [36]. δH (400 MHz, $CDCl_3$) 5.89 (2H, bs, $2 \times NH$) 3.16 (4H, m, $2 \times CH_2NCO$) 2.61 (2H, t, $J = 7.5$ Hz, CH_2NH_2) 2.13 (4H, bm, $2 \times CH_2CO$) 1.61 (6H, m, $2 \times CH_2CH_2CO + NH_2$) 1.46 (6H, m, $CH_2CH_2NH_2 + CH_2(CH_2)_4NH_2 + CH_2CH_3$) 1.27 (4H, m, $CH_2(CH_2)_3NH_2 + CH_2(CH_2)_2NH_2$) 0.87 (3H, t, $J = 7.2$ Hz, CH_3); δC (75.4 MHz, CD_3OD) 173.07, 173.05 42.3, 41.4, 39.6, 36.4, 33.8, 29.8, 26.9, 26.7, 25.3, 23.1, 11.6; *m/z* (%) 285 (17.8, M^+) 269 (8.6) 256 (40.7) 241 (11.3) 227 (21.0) 213 (17.2) 200 (47.6) 196 (10.7) 185 (24.5) 170 (98.3) 142 (52.9) 128 (26.4) 114 (55.4) 100 (64.7) 91 (13.5) 86 (100) 72 (27.6); $C_{15}H_{31}N_3O_2 \cdot H_2O$ requires C 59.4 H 10.9 N 13.8% found C 60.1 H 10.3 N 13.7%.

2.4. 6-Propionamidohexyladipamidopropionamide (*4*)

To a stirred solution of 6-aminohexyladipamidopropionamide (**3**) (1 g, 3.5 mmol) and triethylamine (1 ml, 726 mg, 7.2 mmol) in chloroform (200 ml) under an atmosphere of nitrogen was added propionyl chloride (352 μl, 370 mg, 3.8 mmol) dropwise over ten minutes. Stirring was continued at ambient temperature for a further 24 h, then the resulting suspension was concentrated in vaccuo to around 50 ml and treated with methanol and gentle heating until it became clear. Solid sodium carbonate (5 g) was added to the mixture, which was stirred at ambient temperature for one hour before removal of the inorganic residue by filtration and evaporation in vacuo to dryness. The residual white solid was purified by column chromatography (25% ethanol in dichloromethane Rf = 0.35) to give 6-propionamidohexyladipamidopropionamide (**4**) (810 mg, 68%) $T_m = 175$°C. δH (500 MHz, $CDCl_3$) 5.94 (bs, 1H, N*H*)

Table 1
Effect of temperature on the main amide bands (vs = very strong, s = strong, m = medium, w = weak and vw = very weak. – denotes no obviously apparent polarisation state. π and σ refer to bands with their transition dipole moments parallel and perpendicular, respectively, to the chain axis)

Band position (cm^{-1}), relative intensity and type	Relative dichroism at rt	Effect of increasing temperature up to 175°C	Band assignment and reference
3307 vs σ	∥ vs	Peak broadens and weakens slightly, shifts to higher wavenumbers (by up to ~10 cm^{-1}). No discernible loss of dichroism.	NH stretch [34]
3195 w σ	∥ s	Peak broadens. No discernible loss of dichroism	N–H stretch + amide (I + II) overtone [34]
3058 m σ	∥ vs	Peak broadens, weakens and shifts to higher wavenumbers (by up to ~12 cm^{-1}). No discernible loss of dichroism.	N–H stretch + amide II overtone [34]
1645 vs σ	∥ vs	Peak broadens slightly. No discernible loss of dichroism	Amide I. Mainly CO stretch (+in plane NH deformation + possibly CN stretching) [34]
1556 m π	⊥ w	Peak weakens slightly and shifts to lower wavenumbers (by up to ~7 cm^{-1}). No obvious loss of dichroism.	Amide II. Mainly in-plane NH deformation (+CO and CN stretches) [31,34]
1539 m π	∥ w	Peak weakens slightly and shifts to higher wavenumbers (by up to ~6 cm^{-1}). No obvious loss of dichroism.	Amide II. Mainly in-plane NH deformation (+CO and CN stretches) [31,34]
1370 m π	–	Peak broadens and weakens.	Amide III. CN stretch + in plane NH deformation, coupled with hydrocarbon skeleton [34]. Also CH_3 end group symmetric deformation.
1275 m π	⊥ s	Peak broadens, weakens and shifts to lower wavenumbers (by up to ~5 cm^{-1}). No discernible loss of dichroism.	Amide III coupled with hydrocarbon skeleton [34]
1202 w π	–	Peak broadens, weakens (particularly between 125 and 150°C), and shifts to higher wavenumbers (by up to ~4 cm^{-1}).	Amide III coupled with hydrocarbon skeleton [34] 'Crystalline' band [22,23,30]
695 s σ	⊥ vs	Peak broadens significantly. Some loss of dichroism, but behaviour at high temperatures is obscured by the detector cut-off limit of 650 cm^{-1}.	Amide V. NH out of plane scissoring [34]

5.84 (bs, 1H, N*H*) 5.66 (bs, 1H, N*H*) 3.29 (6H, m, 3 × CH_2N) 2.24 (6H, m, 3 × CH_2C═O) 1.67 (bm, 8H, 2 × CH_2CH$_2$NH +2 × CH$_2$CH$_2$C═O) 1.55 (2H, bm, NHCH$_2$CH_2CH$_3$) 1.35 (4H, m, 2 × CH_2CH$_2$CH$_2$NH)1.17 (3h, t,$J = 7.5$ Hz, O═CCH$_2$CH_3) 0.94 (3H, t,$J = 7.5$ Hz, NHCH$_2$CH$_2$CH_3); δC (75.4 MHz, CD_3OD) 175.8, 174.68, 174.65, 41.1, 41.0, 39.2, 39.1, 35.7, 35.6, 29.2, 29.1, 29.0, 26.43, 26.41, 25.5; *m/z* (%) 341 (14.4)(M^+) 283 (17.3) 255 (21.0) 241 (29.7) 227 (39.6) 214 (17.0) 200 (22.5)170 (100)156 (25.1) 142 (48.8); see Tables 1–3 for IR peaks; HRMS $C_{18}H_{35}N_3O_3$ requires 342.2756 found 342.2758.

2.5. Crystallisation conditions

Single crystals suitable for the polarised μ-FTIR studies were obtained by slow isothermal crystallisation at small supercoolings from methanol solutions. Crystals were grown in the temperature range 7–15°C. The powder samples for the FTIR studies were obtained by placing droplets of oligoamide solution in methanol directly onto a BaF_2 window, and allowing the methanol to evaporate. Powder samples for the X-ray diffraction were crystallised under the same conditions as for the single crystal used in the μ-FTIR studies.

2.6. FTIR

Polarised transmission μ-FTIR spectra were obtained at different temperatures using a Nicolet 860 spectrometer equipped with a NicPlan™ microscope, a 15X, 0.58 NA Cassegrain objective and a gold-grid polariser on a ZnSe substrate. A Linkam FTIR600 hot stage fitted with BaF_2 windows was mounted on the microscope stage to control sample temperature. At each temperature, spectra were obtained in two polarisation directions, corresponding to directions parallel and perpendicular to the long axis of the crystal. 100 scans were collected for each spectrum from 4000 to 650 cm^{-1} at a resolution of 4 cm^{-1}. The resulting single-beam spectra were ratioed against background spectra taken at room temperature with the appropriate polarisation, in order to obtain the polarised single crystal spectra. Water vapour corrections were applied to all the spectra. Baseline corrections were applied to the spectra of some of the weaker peaks (specifically Figs. 6d, 7 and

Table 2
Effect of temperature on the main methylene stretching and scissoring bands (β-CO sym peak is expected at 2868 cm^{-1} [32], but this region is obscured by the overlapping of the two bands at 2858 and 2876 cm^{-1}. sh denotes shoulder)

Band position (cm^{-1}), relative intensity and type	Relative dichroism at rt	Effect of increasing temperature up to 175°C	Band assignment and reference
2957 s σ	∥ s	Peak broadens, particularly between 125 and 150°C.	Tentatively assigned to a Fermi resonance band [33]
2946 s σ	∥ vw	Peak broadens, particularly between 125 and 150°C.	CH_2 α-NH asym. stretch [29]
2933 vs σ	⊥ vs	Peak broadens. There is significant loss of dichroism above 125°C.	CH_2 β-NH asym. stretch [32]
2922 m σ	⊥ w	Behaviour is obscured by the overlapping 2933 cm^{-1} peak.	CH_2 α-CO asym. stretch [32] + CH_3 sym. stretch [31]
2908 m σ	∥ w	Behaviour is obscured by overlapping peaks.	CH_2 γ-NH and β-CO asym. stretch [32]
2876 s σ	–	Peak broadens. There is a dramatic broadening and weakening between 125 and 150°C.	CH_2 α-NH sym. stretch [29,32]
2858 s σ	∥ s	Peak broadens. There is a dramatic loss of dichroism between 125 and 160°C.	CH_2 β-NH and γ-NH sym. stretch [32]
2826 w σ	∥ w	Peak broadens. Behaviour is obscured by overlapping 2858 cm^{-1} peak at high temperatures.	CH_2 α-CO sym. stretch [32]
1474 s σ	∥ vs	Dramatic weakening and broadening between 125 and 150°C.	CH_2 scissoring next to NH group, trans conformation [27–29]
1466 w σ	∥ vw	Weakening and broadening, particularly between 125 and 150°C.	CH_2 scissoring for all methylenes not adjacent to the amide group [28,29]
1417 m σ	∥ vs	Dramatic weakening and broadening between 125 and 150°C.	CH_2 scissoring next to CO group, trans conformation [27–29]

8), for ease of comparison. Transmission FTIR powder studies were undertaken by mounting the Linkam hot stage vertically in a Nicolet Nexus spectrometer, equipped with a liquid nitrogen cooled HgCdTe detector. 32 scans were collected for each spectra from 4000 to 650 cm^{-1} at a resolution of 4 cm^{-1}. The resulting spectra were ratioed against a background spectra taken at room temperature in order to obtain the powder spectra.

One of the problems with obtaining high quality μ-FTIR spectra from this material is the inherent absorption strength of some of the relevant bands, which can saturate at even moderate sample thickness. In many of the spectra (e.g. Figs 3a, 3c, 4a and 4b) there is significant noise and distortion atop some of the stronger bands (notably at ~3300 cm^{-1}). Even though the apparent strength of these bands appears reasonable (ca. 1.5 absorbance units or less), it is likely that in fact these bands have slightly saturated, and that stray light has reduced the apparent absorbance values. This is quite likely, since the spectra were obtained near the edge of the crystal where the thickness was lower. This means that the true values of the band intensities will be slightly higher than those measured from the raw data.

2.7. Powder X-ray diffraction studies

The X-ray diffraction studies were performed at the synchrotron X-ray source at Daresbury Laboratory, UK using beamline 16.2, which operates at the fixed wavelength of 0.1355 nm. The powder samples were heated by placing the powder uncovered on a quartz cover slip on the Linkam hot stage heating block, which was mounted horizontally. In this open arrangement, the sample temperature could not be measured to an accuracy better than ±10°C. Diffraction data were collected using a solid state point detector.

2.8. Differential Scanning Calorimetry (DSC)

DSC scans of the oligoamide crystallised from methanol solutions were run from room temperature to 220°C at a rate of 10°C/min under a N_2 gas flow on a Perkin–Elmer Pyris 1.

3. Results and discussion

The required monodisperse 3-amide oligomer shown in Fig. 1 was synthesised following the procedure outlined in Section 2. Crystallisation of the oligomer from methanol solution at small supercoolings produced thin platelets suitable for polarised μ-FTIR studies. Typical dimensions of the platelets were ~1 × 0.1 × 0.01 mm.

3.1. Differential Scanning Calorimetry (DSC)

A single melting peak was observed at 175.2 ± 0.1°C. The enthalpy of melting was 162 ± 10 J g^{-1}. A small broad endothermic peak with an enthalpy of 9.5 ± 1 J g^{-1} was observed centred at 148.3 ± 0.1°C extending over 20°C; this peak is associated with the Brill transition for this material.

Table 3
Effect of temperature on the 'Brill' and associated bands

Band position (cm^{-1}) and relative intensity	Relative dichroism at rt	Effect of increasing temperature up to 175°C	Band assignment and reference
1327 vw	∥ m	Progressive peak broadening to higher wavenumbers and peak weakening. Above 150°C, this band is not observed.	CH_2 wagging or twist + amide III [22]. 'Regular fold' band [22–24]
1307 vw	⊥ w	Progressive broadening of the peak. Peak is still detectable at 175°C.	CH_2 twisting [30]
1223 vw sh	∥ s	Peak broadens slightly. Abrupt decrease in intensity between 125 and 150°C. No absorbance detectable above 150°C.	CH_2 wagging or twist + amide III [22]. 'Regular fold' band [22–24]
1068 w	∥ s	Dramatic weakening and broadening of the band, particularly between 125 and 150°C. No absorbance detectable above 150°C.	Skeletal C–C stretch [30]
1042 vw	∥ m	Progressive broadening to lower wavenumbers and weakening of the band. Band is only just detectable at 175°C.	Skeletal C–C stretch [30]
1014 vw	∥ m	Progressive broadening to lower wavenumbers and weakening of the band. Band is only just detectable at 175°C.	Skeletal C–C stretch [30]
987 vw	∥ m	Band is very weak, but still observable at 170°C.	CH_2 rocking [30]
906 w	–	Progressive broadening and weakening of the band. Band is detectable at 175°C.	CH_2 rocking [30]
943 m	∥ m	Dramatic decrease in intensity, particularly between 125 and 150°C. Band is only just detectable at 175°C.	C–CO stretch [26,30]. 'Crystallinity' band [22,23,30]

3.2. Powder X-ray diffraction studies

The oligoamide room temperature crystal structure determined by the X-ray powder studies was essentially unchanged from that given in Ref. [18], i.e. $a = 0.490$ nm, $b = 0.533$ nm, c (chain axis) $= 2.850$ nm, $\alpha = 50°$, $\beta = 77°$ and $\gamma = 62.5°$. Upon heating, the intersheet shear of ~40° present in the room temperature structure decreased to a value of ~35° at 175°C, just prior to melting. The Brill transition occurred at 160 ± 10°C. The Brill transition temperature recorded by these X-ray studies appears to be slightly higher than the temperature of 148°C at which the broad endothermic peak is observed in the DSC measurements. This difference is probably due primarily to the inaccuracy incurred in the X-ray measurement set-up. Comparing these results with the Brill transition of 155 ± 5°C reported for this material in Ref. [18], it is likely that $T_B \sim 150$–160°C. Irrespective of the precise value of T_B, it is clear that the material undergoes a Brill transition prior to melting.

3.3. Polarised single crystal FTIR studies

The single crystal chosen for the polarised FTIR studies had nominal dimensions of $\sim 1 \times 0.15 \times 0.01$ mm. The crystal thickness was slightly too thick to perform fully accurate quantitative analysis upon the strongly absorbing bands, however a thinner crystal was not chosen because this would have precluded the observation of the weakly absorbing bands. Multiple optical reflections between the crystal surfaces produced a small amplitude (<0.1 absorbance units) sinusoidal interference fringe in the baseline, with a period of ~600 cm^{-1} in the 25°C spectra. This is consistent with reflection between surfaces separated by ca 6 μm, assuming a refractive index $n = 1.5$. Dampening of this sinusoidal wave occurred at higher temperatures, probably due to expansion and distortion of the crystal, reducing the parallelism of the crystal basal faces. The precise area sampled by the IR beam is shown in Fig. 3a inset.

In the following discussions, the notation π and σ refer to absorption bands for which the transition dipole moments are parallel and perpendicular, respectively, to the chain axis. ∥ and ⊥ states are assigned to vibrations with their transition moments parallel and perpendicular to the crystal long axis (a direction), respectively. Please note, these ∥ and ⊥ directions differ to those documented in the studies on biaxially oriented nylon films, for which ∥ and ⊥ notations are denoted with respect to the hydrogen bonded sheet (i.e. the (010) plane). In addition, it should be borne in mind that the change in intersheet shear from ~40 to 35° upon heating will result in an intrinsic slight decrease in intensity for all the π bands in the single crystal spectra.

Fig. 3a and b shows the corresponding parallel (∥) and perpendicular (⊥) spectra in the range 3600–2600 and 1800–800 cm^{-1} for the oligoamide crystal at temperatures of 25, 50, 75, 100, 125, 150, 160, 170 and 175°C. The

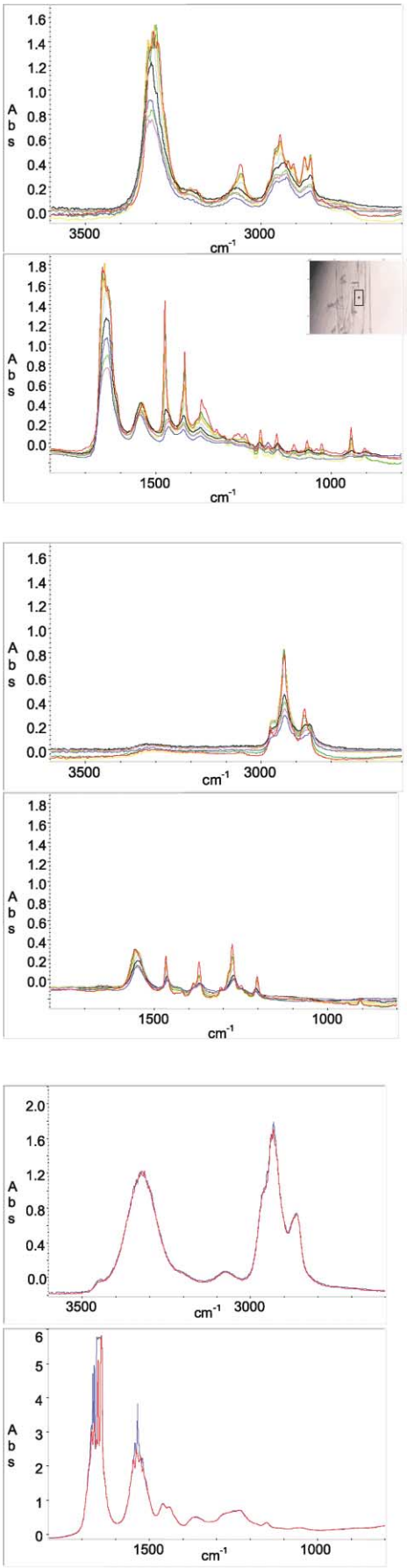

spectra are entirely analogous to that of the nylon 6 6 polymer [25–29,34], except that the spectra are expected to be essentially free from amorphous and fold bands. The ‖ and ⊥ spectra of the melt at 180°C are compared in Fig. 3c. As expected, all dichroism has been lost, and the spectra resemble that of molten nylon 6 6.

3.4. Amide bands

Table 1 lists the main amide bands, their polarisation states, behaviour upon heating and band assignments. All the amide bands occur at frequencies expected for an α-phase nylon 6 6 crystal analogue [26–28]. The variation of peak intensity and position upon heating is also in agreement with previous studies on nylon 6 6 [26,34]. The direction(s) of the essentially linear hydrogen bonds within the crystal will correspond closely to the polarisation direction of the NH stretch (3307 cm^{-1}) and amide I (1645 cm^{-1}) bands (the latter band originates primarily from a carbonyl stretch). Hence any change in hydrogen bond direction would also necessarily involve a change in the dichroism of these bands. Fig. 4a and b compares the ‖ and ⊥ spectra obtained in the NH stretch and amide I regions at 25, 50, 75, 100, 125, 150, 160, 170 and 175°C, respectively. Note that all the different temperature ⊥ spectra run along/close to the baseline in the NH stretch and amide I regions. These figures highlight that both the NH stretch and amide I bands exhibit very strong ‖ dichroism at room temperature; this shows that the hydrogen bonds run predominantly along the long axis of the crystal, in agreement with previous diffraction data [18]. It is immediately apparent from Fig. 4a and b that this very strong ‖ dichroism is retained right up to the crystal melting point for both the NH stretch and amide I bands; since all the ‖ spectra show significant absorption in the NH stretch and amide I region, whilst all the ⊥ scans run along/close to the baseline in these regions. Indeed no discernible absorption is observed in the ⊥ spectra for both the NH-stretch and Amide I region, until melting. Therefore, these figures provide unequivocal proof that the Brill transition in this oligoamide, which occurs at ~150–160°C, prior to melting, cannot involve any significant rearrangement of the sheet hydrogen bond arrangement. The strong ‖ dichroism exhibited by the NH stretch and amide I bands shows that the hydrogen bonds run along the long axis of the crystal at room temperature, and this preferred direction is

Fig. 3. Polarised single crystal μ-FTIR spectra at 25 (red line), 50 (yellow line), 75 (green line), 100 (light brown line), 125 (light blue line), 150 (black line), 160 (light green line), 170 (pink line) and 175°C (blue line). (a) Parallel (‖) spectra between 3600–2600 and 1800–800 cm^{-1} with the polarisation parallel to the crystal long axis. (b) Perpendicular (⊥) spectra between 3600–2600 and 1800–800 cm^{-1} with the polarisation perpendicular to the crystal long axis. (c) ‖ (blue line) and ⊥ (red line) melt spectra at 180°C between 3600–2600 and 1800–800 cm^{-1}. Please note some over-absorption is evident in these spectra particularly at ~3000 cm^{-1} and in the melt spectra in (c), as mentioned in the Section 2.6. Fig. 3a inset shows the crystal region sampled by the IR beam.

retained right up to melting. Appendix A shows how the magnitude of the infrared dichroism can be quantitatively related to the angle of rotation of the chain about its extended axis. The observed dichroism in this data implies that the maximum rotation of the NH groups around the extended chain director, as a function of temperature up to melting, was only about 5°. The dichroic behaviour of the amide bands of this model compound are expected to be entirely analogous to the nylon 6 6 α-phase crystals, since the crystalline structure of these two systems are equivalent. Hence the analogous Brill transition in nylon 6 6 is also highly likely to occur without any significant rearrangement of hydrogen bonds.

The thermal behaviour of the NH-stretch and amide I and II bands are in qualitative agreement with those reported for nylon 6 6 [26], except that no peak at ~3400 cm^{-1} due to non hydrogen-bonded NH stretches develops prior to melting. This is consistent with a ~100% crystalline sample in which there are no amorphous regions.

None of the other amide bands show any significant loss of dichroism upon heating above the Brill transition. Hence, all the data is consistent with a crystalline structure for this oligoamide (and by analogy, nylon 6 6) in which the amide groups are effectively pinned right up to melting. There is no evidence of any amide group reorientation at the Brill transition. Indeed, the only significant changes observed in the amide absorption bands relate to the progressive broadening, weakening and band shifting expected from the reduction in hydrogen bond strength which occurs upon heating (see Table 1) [26].

In contrast, pronounced temperature-induced dichroism changes are seen in the methylene stretching region, particularly at the onset of the Brill transition.

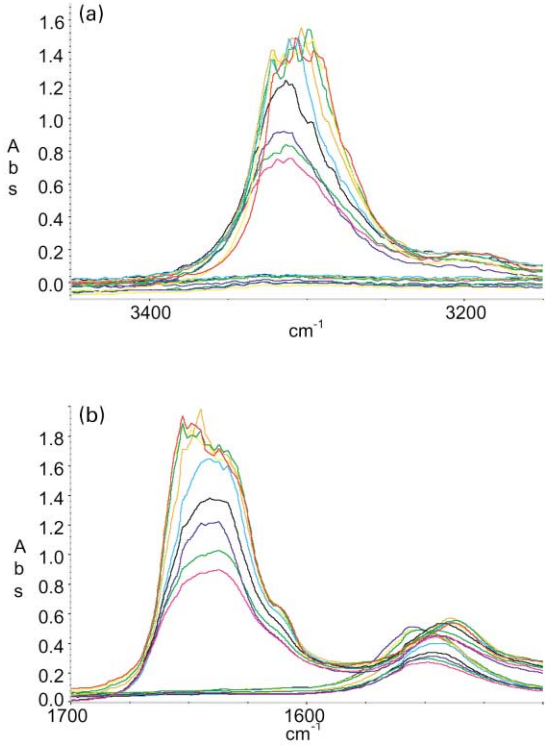

Fig. 4. Comparison of the ∥ and ⊥ spectra at 25, 50, 75, 100, 125, 150, 160, 170 and 175°C. The colour scheme is the same as in Fig. 3. (a) NH stretch region and (b) amide I and II region. Note for both the NH-stretch and amide I region, no absorption is observed in the ⊥ spectra until melting, showing that the amide orientation is essentially invariant. There is some saturation evident in both Fig. 4a and b at the lowest temperatures (25, 50 and 75°C) studied, as mentioned in Section 2.6.

3.5. Methylene stretching region

Fig. 5a and b shows the ∥ and ⊥ spectra, respectively, of the methylene stretching region at 25, 50, 75, 100, 125, 150, 160, 170 and 175°C. Fig. 5c shows the powder spectrum in this region at temperatures of 30, 50, 75, 100, 120, 130, 140, 150, and 160°C. The ∥ and ⊥ spectra are compared at the successive temperatures of 25, 125, 150, 160 and 175°C in Fig. 5d. The band positions, relative intensities and polarisation states of these bands at room temperature are listed in Table 2, along with the band assignments based on previous studies, notably the IR studies on nylon 6 6 by Heidemann and Zahn [29] and the Raman studies on nylon 6 6 by Zimba et al. [32]. Please note, we have assigned the asymmetric stretch of the NH vicinal methylene to the band at 2946 cm^{-1} in accordance with Ref. [29], but not Ref. [32] for which this band was assigned to the peak at 2957 cm^{-1}. This choice was adopted because the small polarisation of the 2946 cm^{-1} band is more in accordance with the lack of polarisation found for the NH vicinal symmetric stretch at 2876 cm^{-1}. We note, however, that Fermi resonance between the symmetric methylene stretches and the overtones of the methylene scissoring complicate this region [32,33]. A detailed quantitative analysis will be the subject of a subsequent paper, so here we state only the trends that are immediately apparent from Fig. 5a–d.

1. There is a general weakening and broadening of the methylene stretching peaks as the temperature increases above 50°C. However in both the ∥ and ⊥ spectra, the most dramatic effects of weakening/broadening are seen in Fig. 5a and b between 125 (light blue line spectra) and 150°C (black line spectra).
2. The weakening of the essentially unpolarised 2876 cm^{-1} peak assigned [29,32] to the NH adjacent CH_2 symmetric stretch is especially marked, particularly between 125 and 150°C (see Fig. 5a and b). A similar effect is found in the powder spectra (see Fig. 5c), where the weakening is particularly evident between 130 (blue line spectrum) and 150°C (black line spectrum).
3. The following bands exhibit pronounced dichroism at room temperature (see Fig. 5d): 2957 cm^{-1} (∥ band tentatively assigned as a Fermi resonance band), 2933 cm^{-1} (⊥ β-NH, asymmetric stretch), and 2858 cm^{-1} (∥ β-NH and γ-NH symmetric stretch

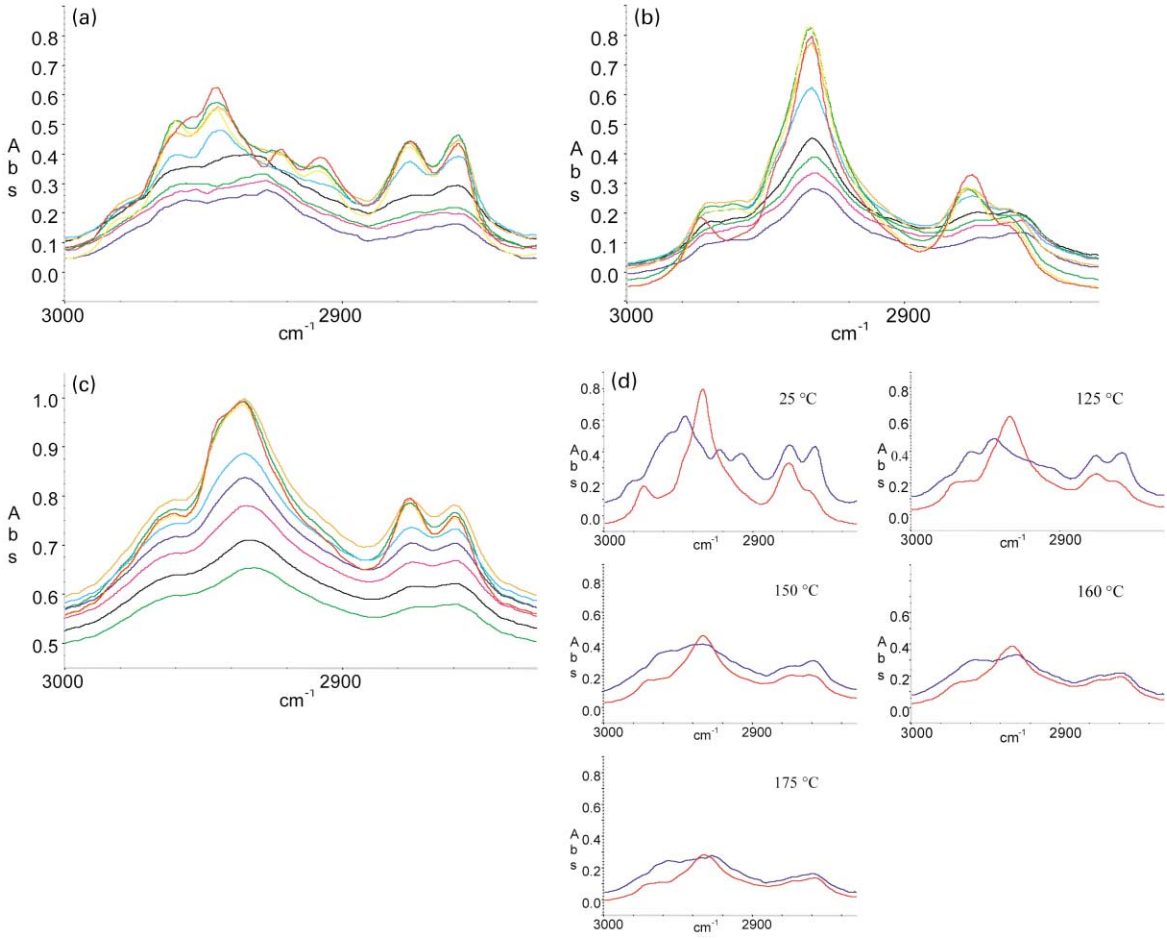

Fig. 5. Spectra of the methylene stretching region. (a) ∥ spectra at 25, 50, 75, 100, 125, 150, 160, 170 and 175°C. (b) ⊥ spectra at 25, 50, 75, 100, 125, 150, 160, 170 and 175°C. The colour scheme is the same for (a) and (b) as in Fig. 3. (c) The corresponding powder spectra at 30 (red line), 50 (yellow line), 75 (green line), 100 (light brown line), 120 (light blue line), 130 (blue line), 140 (pink line), 150 (black line), and 160°C (light green). (d) Successive comparison of the ∥ (blue line) and ⊥ (red line) spectra at 25, 125, 150, 160 and 175°C.

bands). None of the methylene stretches in the diacid unit show any significant dichroism at room temperature. There is a marked reduction in the dichroism shown by the 2858 cm^{-1} peak between 125 and 150°C. At 160°C, no dichroism is discernible. Consequently, at temperatures ≥160°C, none of the symmetric stretch bands show any dichroism; indeed dichroism is only discernible for the bands at 2957 and 2933 cm^{-1} in this temperature range. The asymmetric stretch at 2933 cm^{-1} retains a small dichroism up to melting, however once more the reduction in dichroism is most marked between 125 and 150°C. The ∥ dichroism of the 2957 cm^{-1} band shows the least reduction with temperature.

This data is consistent with the NMR studies on nylon 6 6 of Hirschinger et al. [5] in which it was found that (i) the diamine segments had less librational freedom than the diacid segments at room temperature and (ii) a sudden increase in the librational freedom of the diamine segments occurred at the Brill transition.

3.6. Methylene scissoring region

Fig. 6a and b shows the ∥ and ⊥ spectra of the methylene scissoring region at 25, 50, 75, 100, 125, 150, 160, 170 and 175°C. Fig. 6c shows the corresponding powder spectra at 30, 50, 75, 100, 120, 130, 140, 150, and 160°C. The ∥ and ⊥ spectra are compared at the successive temperatures of 125, 150 and 175°C in Fig. 6d. The band positions, relative intensities and polarisation states of these bands at room temperature are listed in Table 2, along with the band assignments based on previous studies. This region exhibits three clearly distinguishable peaks at 1474, 1466 and 1417 cm^{-1}, together with shoulders at ~1460 and ~1427 cm^{-1}.

Both the 1474 and 1417 cm^{-1} bands, which have been assigned to *trans*-conformation methylene scissoring modes adjacent to the NH and CO groups [28,29], show very strong ∥ dichroism at room temperature (see Fig. 6a). The dichroism is reduced as the temperature is raised, however at 175°C, the ∥ dichroism of both bands is still

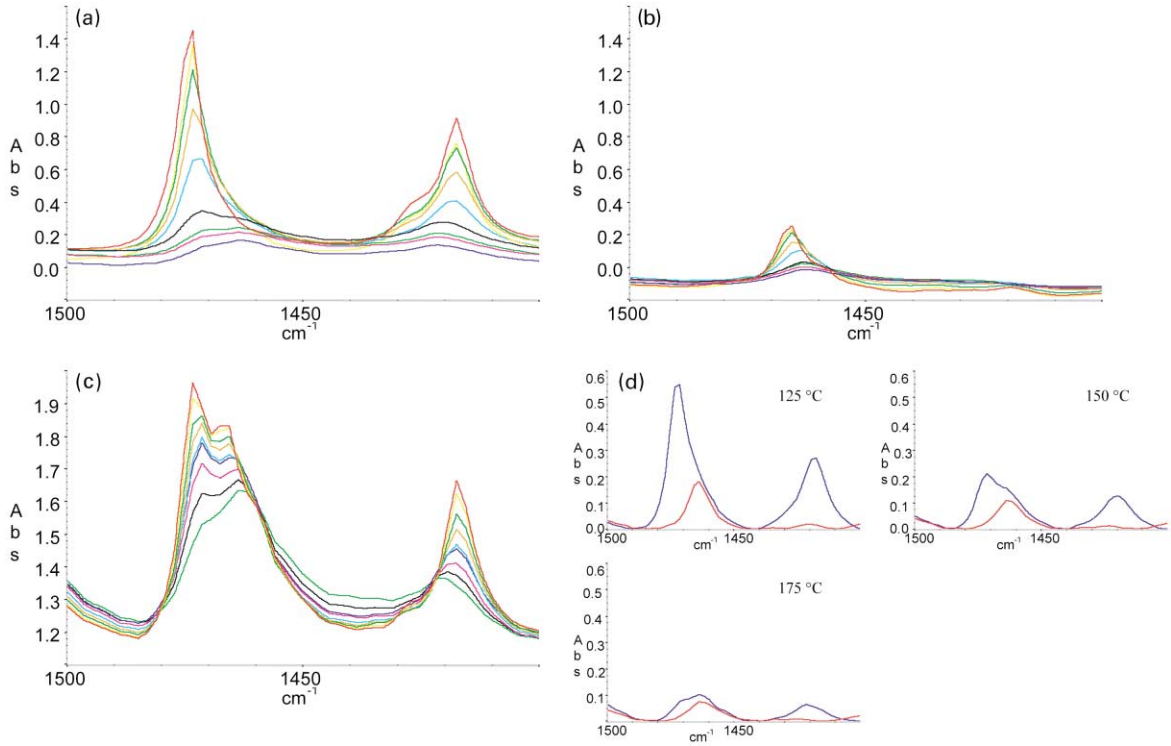

Fig. 6. Spectra of the methylene scissoring region. The colour scheme is the same as in Fig. 5. (a) ∥ spectra at 25, 50, 75, 100, 125, 150, 160, 170 and 175°C. (b) ⊥ spectra at 25, 50, 75, 100, 125, 150, 160, 170 and 175°C. (c) The corresponding powder spectra at 30, 50, 75, 100, 120, 130, 140, 150, and 160°C. (d) Successive comparison of the ∥ (blue line) and ⊥ spectra (red line) at 125, 150 and 175°C. Baseline corrections have been applied to (d).

clearly observable. Both these amide vicinal bands show a pronounced weakening and broadening with temperature (see Fig. 6a and b), and these effects are particularly marked in the temperature range 125–150°C (compare the light blue and black line spectra in Fig. 6a and b and see Fig. 6d); this temperature range corresponds to the onset of the Brill transition. The peak at 1466 cm^{-1}, which is attributed to non-amide vicinal CH_2 scissoring, shows a similar, though less marked effect. All these intensity changes are mirrored in the powder studies (see Fig. 6c).

It has previously been found that the scissoring modes of the amide vicinal methylenes depend upon the conformation relative to the amide group. In particular, the NH vicinal peak at 1474 cm^{-1} and the CO vicinal peak at 1417 cm^{-1} occur at ~1440 cm^{-1} if the amides are rotated out of the alkane plane so that the trans conformation is lost [27–29]; this occurs in the γ-phase of nylons [28]. There is no evidence of a new peak developing at ~1440 cm^{-1} prior to melting, which would have been indicative of a twisted amide conformation, although a small peak may be present but swamped by the overlapping and broadening 1466 and 1417 cm^{-1} bands. Upon melting, however, an intense broad peak centred around 1440 cm^{-1} occurs (see Fig. 3c). This provides further evidence that the amides remain essentially in/close to the alkane plane until melting occurs. Consequently, the methylene scissoring data is consistent with a Brill transition mechanism in which the amide vicinal methylenes experience larger amplitude librational motion, whilst still retaining a largely all-*trans* amide–alkane torsion angle.

In summary, the evidence supports a model for the Brill transition in nylon 6 6 in which the methylene units undergo enhanced librational motion, but the amide groups remain effectively pinned up to melting. We envisage the transition occurring as follows. At room temperature, the hydrogen bonds within the sheets hold the chains further apart than the intersheet separation which is controlled by van der Waals forces (i.e. $d_{(100)} > d_{(010)/(110)}$). With increasing temperature, the methylene units undergo greater librational motion, causing the intersheet separation to increase. At the Brill transition, the interchain separations become equal, and the methylene units undergo enhanced librational motion. Increasing temperature will cause further increased methylene motion, and the interchain separations will increase equally until the hydrogen bonds break and the material melts. The enhanced methylene motion above T_B would be expected to produce a lower entropy of melting than occurs for nylons that do not undergo a Brill transition, e.g. nylon 6. Please note that we do not rule out the occurrence of a three-dimensional arrangement of hydrogen bonds in related nylons that form a hexagonal or nearly hexagonal structure. In these structures, the interamide distances are equivalent, or nearly so, and hence hydrogen bonds of similar strength can be formed in the trigonal directions. In nylon 6 6, however, the pronounced intersheet shear results in intersheet amide

distances that are too great for effective hydrogen bond formation.

3.7. 'Fold', 'amorphous' and 'crystallinity' bands

The bands at 1327 and 1223 cm^{-1} have been identified as 'regular fold' bands [22–24]. Those at 1180 and 1144 cm^{-1} have been designated as 'amorphous' bands [22,23], whilst bands at 1202 and 943 cm^{-1} have been identified as 'crystalline' [22,23,30]. Therefore, we would not expect to observe the peaks at 1327, 1223, 1180 and 1144 cm^{-1} in the spectra of our extended chain, essentially 100% crystalline oligomer. However, all these peaks are present to varying extents, as detailed below.

The 'regular fold' bands at 1327 and 1223 cm^{-1} have been tentatively assigned as a coupling of the vicinal NH methylene twisting and wagging modes with the amide III mode [22]. The presence of both these parallel bands in our spectra show that these bands cannot be uniquely assigned as fold bands. However the decreased intensity of the 1223 cm^{-1} band, compared to that of the 1327 cm^{-1}, suggests that the proportion of fold character in this band is greater than that of the 1327 cm^{-1}. Vasanthan et al. [20] have designated these bands, amongst others, as 'Brill' bands. Further discussion detailing their temperature behaviour may be found under Section 3.8.

Both the 'amorphous' bands at 1180 and 1144 cm^{-1} (tentatively assigned as a methylene CO twist [30]) are observed, and both show ∥ polarization at all temperatures below the melting point. The 1180 cm^{-1} band shows only small changes upon heating up to 125°C, but undergoes a >2-fold increase in intensity between 125 and 150°C; thereafter the absorbance increases only marginally until melting (compare the light blue line (125°C) and black line (150°C) spectra in Fig. 7a). The behaviour of the weaker 1144 cm^{-1} band is harder to discern because it is obscured at temperatures ≥100°C by its overlap with the broadening 1155 cm^{-1} band. Although these 'amorphous' bands are significantly weaker than in nylon 6 6, their occurrence and their polarisation states indicate that they are not uniquely ascribed to amorphous regions, in agreement with the findings of Quintanilla et al. [25]. However, it is also possible that the end-groups in the oligoamide contribute to some or all of these features.

The 'crystallinity' band at 943 cm^{-1}, which has been assigned as a C–CO stretch by most studies [26,30], shows a very pronounced parallel dichroism at room temperature. The intensity of this band weakens with temperature, and this is particularly pronounced between 125 and 150°C; a greater than two-fold intensity decrease occurs in this temperature range, so that only a small absorbance is detected at 150°C (compare the light blue line (125°C) and black line (150°C) spectra in Fig. 7b). At 175°C, the band has virtually disappeared. These findings are duplicated in the powder studies. The other 'crystallinity' band at 1202 cm^{-1} also shows a dramatic decrease in intensity between 125 (light blue line spectra) and 150°C

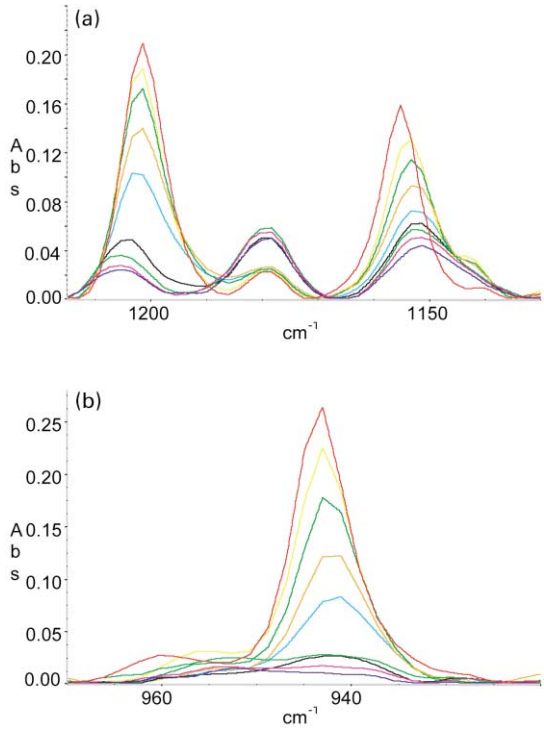

Fig. 7. Spectra showing amorphous and crystalline bands at 25, 50, 75, 100, 125, 150, 160, 170 and 175°C. The colour scheme is the same as in Fig. 3. (a) ∥ spectra of the 'amorphous' 1180 cm^{-1} band, 'crystalline' 1202 cm^{-1} band and 1155 cm^{-1} band. Note the contrasting thermal behaviour of the 1155 cm^{-1} peak which shows gradual changes with temperature compared to the 1202 'crystalline' and 1180 'amorphous' peak which show dramatic decreases, and increases, in intensity respectively between 125 and 150°C. (b) ∥ spectra of the 943 cm^{-1} 'crystallinity' band. Baseline corrections have been applied to (a) and (b) for ease of comparison.

(black line spectra), accompanied by a small shift (~4 cm^{-1} at 175°C) to higher wavenumbers, as shown in Fig. 7a.

These findings support the conclusions of Quintanilla et al. [25], i.e. that the 943 cm^{-1} peak is correlated with the total proportion of trans conformation in the crystalline and amorphous regions, rather than the degree of crystallinity. Similarly the amorphous 1144 cm^{-1} peak is correlated with the total proportion of gauche conformation, rather than the extent of amorphous regions. Certainly the dramatic intensity increase of the 'amorphous' peak accompanied by the dramatic intensity decrease of the 'crystalline' peaks in the Brill temperature range are consistent with the enhanced *trans/gauche* isomerisation that is expected at these temperatures.

The contrasting behaviour of the amorphous and crystalline peaks at 1180 and 1202 cm^{-1}, which show marked intensity increases/decreases, respectively, between 125 and 150°C, compared to the behaviour of the nearby 1155 cm^{-1} peak, which shows only gradual changes with temperature, are evident in Fig. 7a.

3.8. 'Brill' bands

A recent paper by Vasanthan et al. [20] described the

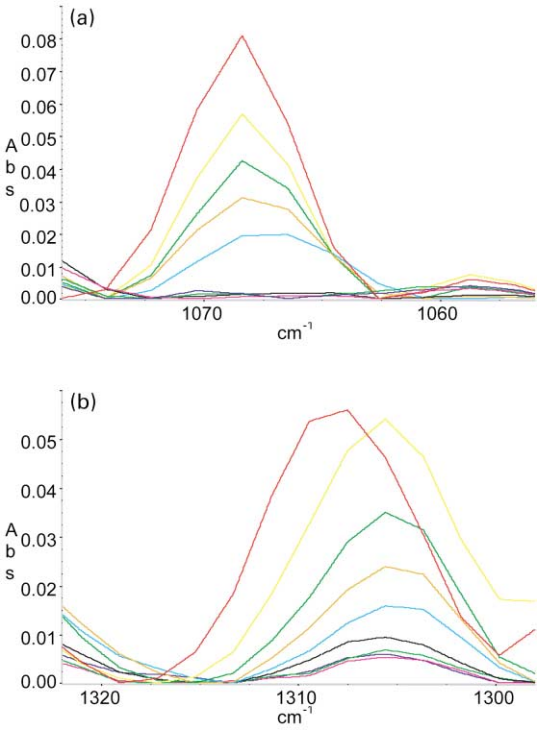

Fig. 8. Spectra illustrating the behaviour of 'Brill' bands [20] at 25, 50, 75, 100, 125, 150, 160, 170 and 175°C. The colour scheme is the same as in Fig. 3. (a) Spectra of the $\parallel$ 1068 cm^{-1} band. Note the abrupt disappearance of this band between 125 and 150°C. (b) Spectra of the $\perp$ 1303 cm^{-1} Brill band, for which we detect a small residual absorbance up to melting. Baseline corrections have been applied to (a) and (b) for ease of comparison.

abrupt disappearance of a number of weaker bands, viz. 1329, 1303, 1224, 1065, 1042, 1014, 987 and possibly 906 cm^{-1}, for melt crystallised nylon 6 6 between 160 and 180°C, i.e. coinciding with the temperature region expected for the Brill transition region. These bands were designated 'Brill bands'. In the spectra of the nylon 6 6 3-amide, all these bands do undergo a significant weakening between 125 and 150°C, and we can detect no absorbance for the 1068, 1223 and 1327 cm^{-1} bands above 150°C in out data set. However our data shows that the very weak bands we observe at 1307, 1042 and 906 cm^{-1} at 25°C retain a small residual absorbance up to melting, whilst the very weak 1014 cm^{-1} band may do so as well, i.e. their behaviour is similar to that of the crystallinity band at 943 cm^{-1} (see Fig. 7b). Similar findings were obtained from the powder spectra, however further more detailed and quantitative studies on this oligoamide are required on these weak bands before definitive statements can be made. Details of these 'Brill' bands, their polarization states, their changes between 125 and 150°C and their assignments based on previous studies are listed in Table 3. The typical behaviour of the bands that disappear at T_B is shown in Fig. 8a taking the 1068 cm^{-1} peak as the example, whilst Fig. 8b shows the thermal behaviour of the peak at 1307 cm^{-1}, a Brill band for which we can detect a small residual absorbance up to melting.

4. Conclusions

1. The extensive parallel dichroism exhibited by the NH stretch and amide I bands is retained right up to the melting point of 175.2°C. This proves that the Brill transition, which occurs at 150–160°C for this material, does not involve a significant rearrangement of hydrogen bonds (quantitative analysis shows that there is $<5°$ rotation of the N–H bonds about the chain axis prior to melting). Since the crystalline behaviour of this model compound is entirely analogous to that of nylon 6 6, the Brill transition in this polymer is also expected to occur without a hydrogen bond rearrangement.
2. The methylene stretching and scissoring regions show dramatic changes in intensity and spectral width at the onset of the Brill transition. This thermal behaviour is more marked for the methylene units adjacent to the N–H groups. A pronounced loss in dichroism also occurs for many of the methylene stretching bands between 125 and 150°C. These findings are consistent with a Brill transition mechanism in which the methylene units undergo enhanced motion, and are in agreement with NMR studies [5] in which the methylenes in the diamine unit were found to be more constrained than those in the diacid unit until T_B was reached.
3. The presence of so-called 'amorphous' and 'fold' bands in our essentially 100% crystalline, chain extended material indicates that these classifications are an oversimplification. The chain conformations giving rise to these bands are expected to be far more prevalent in the amorphous, and fold regions, however their presence is not wholly confined to these locations.
4. Our data set indicates that some 'Brill' bands, notably the 1068, 1223 and 1327 cm^{-1} peaks do disappear at the Brill transition, yet others appear to retain a small residual absorbance up to melting.

Acknowledgements

We would like to thank the EPSRC mass spectroscopy service at Swansea University for the accurate mass spectroscopy data. We acknowledge the provision of time on DARTS, the UK national synchrotron radiation service at the CLRC Daresbury Laboratory, through funding by the EPSRC. SJC would like to acknowledge ICI for the kind provision of her lectureship.

Appendix A. Calculation of chain rotation angles from infrared dichroic ratios

It is possible to quantify the extent of rotation about the chain long axis that occurs on heating the sample. Fig. A1 summarises the experimental geometry. The chain director r lies in the b^*c^* plane, inclined at an angle θ from the c^* axis. The transition dipole moment for an arbitrary vibration lies

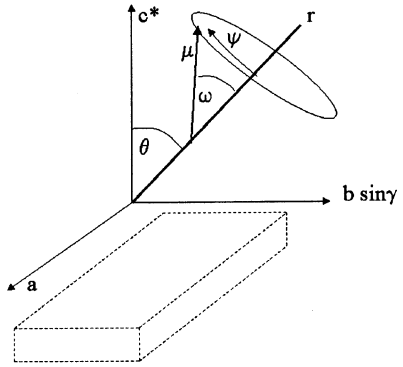

Fig. A1. Schematic of chain orientation geometry. The extended chain director (r) lies at an angle θ to the c^* axis, in the b^*c^* plane. The vibrational dipole (μ) lies at an angle ω to r, and points in a direction governed by chain rotation about r. In the oligoamide at rt, $\theta = 40°$, $\omega = 90°$ (the N–H stretch), and μ lies parallel to the a axis ($\psi = 0$).

at an angle ω to the chain director, and its direction in space is determined by rotation about the chain director (ψ). For the N–H stretch, and amide I bands, it is assumed that $\omega = 90°$, and that at room temperature the chains are rotated so that the N–H and C=O transition dipoles lie parallel to the a axis (defined as $\psi = 0$).

The dichroic ratio D is given by the ratio of band absorbances (A) measured with light polarised parallel to a and $b^*\sin\gamma^*$ ($= b \sin\gamma$) ($D = A_a/A_{b\ \sin\beta}$). If all dipoles are aligned parallel to a, and the IR beam is perfectly polarised in the b^*c^* plane, then D should be infinite. Our requirement is to compute the rotational angle ψ from the observed dichroic ratio and the known tilt angle θ. This is easily achieved using a simple coordinate transformation [37]. The a, $b \sin\gamma$ and c^* components of the transition dipole μ are then given by Eq. (A1).

$$\begin{bmatrix} \mu_{b\ \sin\gamma} \\ \mu_a \\ \mu_{c^*} \end{bmatrix} = \begin{bmatrix} \cos(\theta) & 0 & \sin(\theta) \\ 0 & 1 & 0 \\ -\sin(\theta) & 0 & \cos(\theta) \end{bmatrix} . \begin{bmatrix} \mu \sin(\omega)\sin(\psi) \\ \mu \sin(\omega)\cos(\psi) \\ \mu \cos(\omega) \end{bmatrix} \tag{A1}$$

Note the slight difference in coordinate system compared with reference [37]; here the dipole angle is ω, not β, and here $\psi = 0$ is defined by the dipole moment lying in the ab plane rather than the b^*c^* plane.

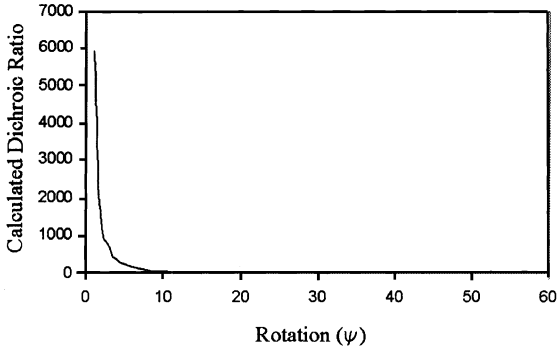

Fig. A2. Calculated dichroic ratio as a function of ψ under the geometry defined by Fig. A1 and its caption.

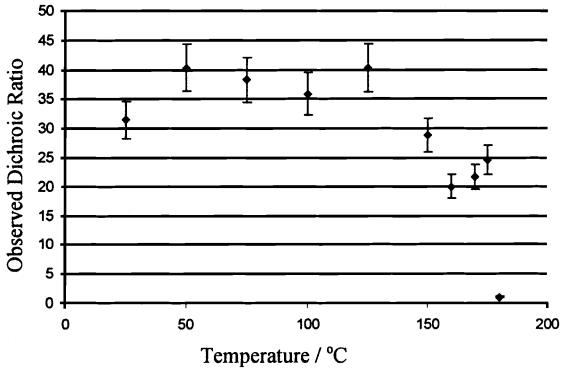

Fig. A3. Measured dichroic ratio for the N–H stretch near 3300 cm^{-1} as a function of temperature. The non-infinite value of D at 25°C implies that there is a non-zero scalar product of the transition dipole and the IR electric field when the IR beam is nominally polarised in the b^*c^* plane.

The infrared absorbance is given by the square of the dipole moment component along a given axis. Bearing in mind that $\omega = 90°$, we find that:

$$D = \mu_a^2/\mu_{b\ \sin\gamma}^2 = \frac{\cos^2(\psi)}{\cos^2(\theta)\sin^2(\psi)} \tag{A2}$$

This is the desired relation between dichroic ratio and rotation about the chain director, on the assumption that all chains undergo the same rotation. The analysis could be readily extended to account for an ensemble of molecules exhibiting a continuous rotational distribution function, but this is not necessary for the purposes of this work [37].

Fig. A2 shows the calculated dichroic ratio as a function of rotation ψ, assuming that the tilt angle $\theta = 40°$. Upon heating this tilt angle changes, becoming ~35° at 175°C, but we ignore this change for the purposes of this work, since the effect is rather small. Rotation of just 10° causes a very significant drop in D which should be easily observed using IR dichroism. Note however that Fig. A2 implies that the dichroic ratio should tend to infinity as the rotation approaches zero, whereas this is not observed in the experimental data. Fig. A3 shows the variation in observed dichroic ratio as a function of temperature for the N–H stretching band near 3300 cm^{-1}. Even at room temperature the dichroic ratio is not infinite ($D \sim 40$) and it decreases with increasing temperature ($D \sim 20$ and 1 at 160 and 180°C, respectively). The finite dichroic ratio at room temperature arises because the vibrational dipole and the electric field vector are not mutually orthogonal when the IR beam is nominally polarised in the bc^* plane. This in turn could be due to several factors.

1. The N–H dipole moment does not lie perfectly parallel to a.
2. The crystal is not aligned perfectly in the polarised IR beam.
3. The IR beam is being focused rather than collimated in

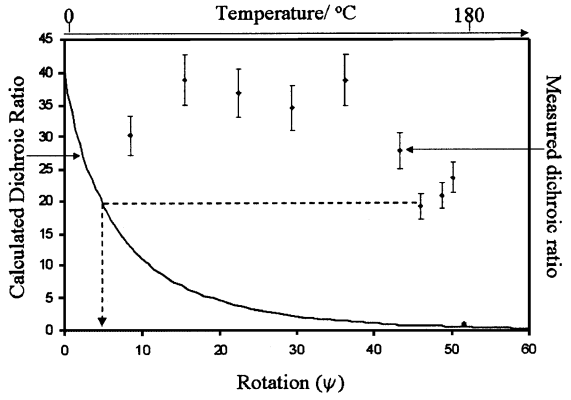

Fig. A4. Plot of calculated dichroic ratios after correction for the angular offset ϵ. The observed dichroic ratios are superimposed as a function of temperature. The dichroic ratio does not fall below 20 before melting occurs, which implies that the maximum rotation of the N–H bonds about the chain axis is ca. 5°.

the crystal, so the selected polarisations are not perfectly parallel to the a and b^* sin γ^* ($= b$ sin γ) axes.

4. Crystal imperfections cause scattering and depolarisation.
5. The birefringent nature of the crystal causes some inherent depolarisation of the beam.

Correcting the data for all of these effects is non-trivial and is beyond the scope of this study. Instead we make a crude, first-order correction which simply assumes that all of the effects above can be collected into a single term, namely a constant angular offset (ϵ) about the c^* axis. This offset implies that when the IR beam is nominally polarised in the a^*c^* plane (or the b^*c^* plane), the true plane of polarisation is actually rotated through ϵ degrees about the c^* axis. This accounts for the non-infinite value of D. The appropriate value of ϵ can be calculated from the maximum observed dichroic ratio, using $D_{max} = \cos^2(\epsilon)/\sin^2(\epsilon)$. From our data we find that $\epsilon \sim 9°$.

Fig. A4 displays the predicted dichroic ratios after correction to account for the additional angular offset of the electric field, and superimposed on this plot are the observed dichroic ratios as a function of temperature. This plot shows that even at temperatures of 160°C, $D > 20$, which implies that the chains have rotated a maximum of about 5° about their long axis. Therefore, no major rearrangement of hydrogen bonds can be inferred from the infrared measurements.

References

[1] Brill R. J Prakt Chem 1942;161:49.
[2] Holmes DR, Bunn CW, Smith DJ. J Polym Sci 1955;17:159.
[3] Cannon CG, Chappel FP, Tidmarsh JI. J Text Inst 1963;54:210.
[4] Colclough ML, Baker R. J Mater Sci 1978;13:2531.
[5] Hirschinger J, Miura H, Gardner KH, English AD. Macromolecules 1990;23:2153–69.
[6] Itoh T, Yamagata T, Hasegawa Y, Hashimoto M, Konishi T. Jpn J Appl Phys 1996;35:4474–5.
[7] Scmidt GF, Stuart HA. Naturforsch 1958;13A:222.
[8] Olf HG, Peterlin A. J Polym Sci A2 (Polym Chem) 1971;9:1449.
[9] Atkins EDT, Hill MJ, Veluraja K. Polymer 1995;36:35.
[10] Jones NA, Cooper SJ, Atkins EDT, Hill MJ, Franco L. J Polym Sci Pol Phys 1997;35:675–88.
[11] Jones NA, Atkins EDT, Hill MJ, Cooper SJ, Franco L. Polymer 1997;38:2689–99.
[12] Atkins EDT, Hill MJ, Jones NA, Cooper SJ. J Polym Sci Pol Phys 1998;36:2401–12.
[13] Cooper SJ, Atkins EDT, Hill MJ. Macromolecules 1998;31:5032–42.
[14] Ramesh C, Keller A, Eltink SJEA. Polymer 1994;35:2483–7.
[15] Xenopoulos A, Wunderlich B. Colloid Polym Sci 1991;269:375–91.
[16] Starkweather HW, Jones GA. J Polym Sci, Poly Phys Ed 1981;19:467.
[17] Starkweather HW, Whitney JF, Johnson DR. J Polym Sci 1963;A1:715.
[18] Cooper SJ, Atkins EDT, Hill MJ. J Polym Sci B (Polym Phys) 1998;36:2849–63.
[19] Cooper SJ, Atkins EDT, Hill MJ. Macromolecules 1998;31:8947–56.
[20] Vasanthan N, Murthy NS, Bray RG. Macromolecules 1998;31: 8433–5.
[21] Itoh T. Jpn J Appl Phys 1976;15:2295–306.
[22] Koenig JL, Itoga M. J Macromol Sci, Phys 1972;B6:327–42.
[23] Koenig JL, Agboatwalla MC. J Macromol Sci, Phys 1968;B2:391–420.
[24] Canon CG, Harris PH. J Macromol Sci, Phys 1969;B3:357–64.
[25] Quintanilla L, Rodriguez-Cabello JC, Pastor JM. Polymer 1994;35:2321–8.
[26] Garcia D, Starkweather HR. J Polym Sci, B (Polym Phys) 1985;23:537–55.
[27] Miyake A. J Polym Sci 1960;44:223–32.
[28] Matsubara I, Magill JH. Polymer 1966;7:199–215.
[29] Heidemann G, Zahn H. Makromol Chem 1963;62:123.
[30] Jakeš J, Krimm S. Spectrochim Acta 1971;27A:19–34 see also p. 35–63.
[31] Sandeman I. Proc R Soc London 1955;A232:105–13.
[32] Zimba CG, Rabolt JF, English AD. Macromolecules 1989;22: 2863–7.
[33] Abbate S, Zerbi G, Wunder SL. J Phys Chem 1982;86:3140–9.
[34] Cannon CG. Spectrochim Acta 1960;16:302–19.
[35] Johnson DH. J Chem Soc 1958:1624–8.
[36] Zahn H, Prakash-Garg O. Kolloid-Z Z Polym 1996;208:132–7 [Chem Abs 1966:65:5361a].
[37] Everall N. Spectroscopy 2000;15:38–46.